



Qualitative and quantitative analysis of patellar vascular anatomy by novel three-dimensional micro-computed-tomography: Implications for total knee arthroplasty

Dingyu Wang^{a,b}, Zhongcheng Shen^{a,b}, Dong Jiang^b, Xu Li^a, Xuan Fang^a, Huijie Leng^{c,*}, Weiguang Zhang^{a,*}

^a Department of Human Anatomy and Histology and Embryology, Peking University, Beijing 100191, PR China

^b Institute of Sports Medicine, Beijing Key Laboratory of Sports Injuries, Peking University Third Hospital, Beijing 100191, PR China

^c Department of Orthopedics, Peking University Third Hospital, Beijing 100191, PR China

ARTICLE INFO

Article history:

Received 1 December 2018

Received in revised form 14 January 2019

Accepted 1 February 2019

Keywords:

Vascular anatomy

Patella

Micro-CT

Total knee arthroplasty

Blood supply

Intraosseous

ABSTRACT

Background: The blood supply of the patella is highly related to patellofemoral complications in total knee arthroplasty. The purpose of this study was to determine (1) the dominant blood supply for the patella and (2) the anatomic characteristics of the extraosseous and intraosseous vascularity of the patella.

Methods: In 13 fresh cadaveric knees, the femoral arteries were cannulated and perfused with a lead-based contrast agent. Patellae were harvested and scanned with a micro-computed-tomography scanner. The three-dimensional microarchitecture of the vascularity was reconstructed and evaluated. For the volumetric analysis, the vessel densities of the anterior, central and subchondral sides were compared.

Results: A well-anastomosed prepatellar vascular network was found to cover the anterior surface of the patella, with main arteries from multiple directions, yielding 18.8 ± 3.1 (standard deviation) intraosseous branches into the patella. Along the intraosseous branches of the prepatellar vascular network, vessel density decreased ($P < 0.001$) by $0.54 \pm 0.29\%$ on the anterior side, $0.40 \pm 0.24\%$ on the central side and $0.23 \pm 0.19\%$ on the subchondral side. Arteries in the infrapatellar fat pad produced 5.1 ± 1.8 intraosseous branches, mainly located in the distal apex. Almost no arteries penetrated into the patella from the quadriceps tendon, patellar ligament or medial/lateral retinaculum.

Conclusion: The prepatellar vascular network is the dominant blood supply. Close exposure and extensive dissection around the patella should be avoided to preserve the prepatellar vascular network. The infrapatellar fat pad was recommended to be preserved when a lateral reticulum release was performed.

© 2019 Elsevier B.V. All rights reserved.

1. Introduction

Patellofemoral complications occur at a rate of five to 50% after total knee arthroplasty (TKA), including anterior knee pain, osteonecrosis, stress fracture and prosthesis loosening, and account for 12% of revision TKAs [1–3]. Iatrogenic disruption of the patella blood supply during TKA has been identified as a possible contributing factor to patellofemoral complications [1,2], especially the lateral release which was associated with postoperative patella fracture and osteonecrosis [4–7]. Therefore,

* Corresponding authors.

E-mail addresses: lenghj@bjmu.edu.cn (H. Leng), zhangwg@bjmu.edu.cn (W. Zhang).

investigation into the vascularization in the patella was necessary to better understand patella vascular anatomy for improvement of the TKA and to reduce the degree of the complications.

It is widely accepted that the knee joint blood supply is derived from six arteries: the supreme genicular, the medial and lateral superior genicular, the medial and lateral inferior genicular, and the anterior tibial recurrent arteries [8]. Branches of these arteries form an anastomotic ring around the patella, supplying blood to the tendons, ligaments, retinaculum, synovial tissue and patella. However, inconsistencies in the intraosseous arterial contribution have been reported in relevant studies [9–11]. The contradictory results are likely due to differences in the methodologies used; all of these previous studies utilized two-dimensional rather than three-dimensional (3D) imaging or sectioning. Neither radiography nor magnetic resonance imaging (MRI) can offer high-resolution images, and qualitative descriptions are not sufficient for illustrating the primary blood supply and the blood vessel distribution of the patella.

The recent development of micro-computed-tomography (micro-CT) has allowed the examination of bone architecture and vascularity at the 10- to 20- μm scale. Micro-CT scanning has been successfully used in animal models [12] and the human femoral head and lunate [13,14]. This technique enables the accurate localization of the arterioles within a 3D structure and the calculation of the volume of the trabecular bone and intraosseous vessels without the need for decalcification or dissection.

The purpose of this study was to reconstruct the 3D vascular microarchitecture of the patella by micro-CT and to better determine, both qualitatively and quantitatively, (1) the dominant blood supply source for the patella and (2) the anatomic characteristics of the extraosseous and intraosseous vascularity of the patella. A better understanding of the vascularity of the patella will allow for the safe planning of surgeries, potentially avoiding areas that contain critical nutrient-supplying vessels.

2. Material and methods

2.1. Specimen preparation

An IRB approval was granted for this study. The ages of the donors ranged from 45 to 93 years (Table 1). Specimens with lower-extremity trauma, previous knee surgery, paralysis, vascular disease including atherosclerosis, diabetes mellitus, skeletal deformities, leukemia and long stays in bed before death were excluded.

Lead oxide (Pb_3O_4 , Sinopharm Chemical Reagent Beijing Co., Ltd.) was used as contrast agent [15], which was ground into particles of less than 40 μm and suspended in turpentine oil (Chemical Reagent Beijing Co., Ltd.) at ratios of 1 g:1.5 ml, 1 g:1 ml and 1 g:0.5 ml [16,17]. The femoral arteries in the femoral triangle were cannulated and perfused with heparinized saline and then the contrast agent (90 ml of 1 g:1.5 ml, 60 ml of 1 g:1 ml and 15 ml of 1 g:0.5 ml). A midline longitudinal skin incision on the knee was made, and successful perfusion was confirmed. The connective tissue above the patella was opened in layers. The thin layer on the patella containing the prepatellar vascular network was finally exposed and carefully preserved. Findings related to the vascular anatomy were recorded, and photographs were taken. Then, the tendons and retinaculum were dissected, and the patella was harvested. Cartilage degeneration was evaluated according to the Outerbridge classification [18].

2.2. Specimen scanning and analysis

Specimens were scanned twice using a micro-CT scanner (Inveon, Siemens Ltd., USA). The primary scanning, with a voxel size of 52.30 μm , was performed on the whole patella to obtain a general view of the intraosseous vascular pattern. The acquisition protocols for primary scanning were as follows: CT scan set-up: total rotation (degrees) = 360, rotation steps = 360; X-ray detector set-up: transaxial = 2048, axial = 2048, exposure time = 1500 ms, binning = 1; system magnification: low; and X-ray tube set-up: voltage = 80 kV, current = 500 mA. The down-sampling factor used in the reconstruction was 2. The extraosseous and intraosseous

Table 1
Cadaveric information and patella conditions.

Age (years)	Gender	Side	Patella height (mm)	Cartilage thickness at MF (mm)	SBP thickness at MF (mm)	Cartilage thickness at LF (mm)	SBP thickness at LF (mm)
93	Male	R	25.8	3.4	0.44	3.6	0.48
51	Male	L	26.0	3.4	0.42	4.8	0.62
61	Male	L	22.5	3.1	0.33	3.6	0.90
45	Male	R	23.2	4.8	0.70	5.2	0.87
75	Male	R	24.1	3.9	0.42	4.3	0.56
80	Male	L	24.3	3.5	0.37	3.2	0.42
57	Male	R	23.4	3.6	0.51	4.2	0.57
71	Female	R	17.6	2.3	0.53	0.37	0.60
72	Male	L	23.9	3.4	0.45	5.0	0.65
50	Male	L	23.5	4.0	0.55	5.5	0.70
68	Male	R	25.4	2.4	0.42	3.3	0.82
57	Male	L	23.0	3.4	0.55	4.1	0.50
77	Female	L	19.5	1.9	0.51	0.42	1.1

L, left; LF, lateral facet; MF, medial facet; R, right; SBP, subchondral bone plate.

vascular anatomy of the patella was evaluated. Patellar height as well as subchondral plate thickness and cartilage thickness in the medial and lateral facets were measured [19].

For whole patella, the size exceeded the size of the high-resolution scanning field; patellae were then divided into six parts using a low-speed saw (CanNeed-LSS-100), which did not cause bone structure destruction near the sawing site (Figure 1(a)) and every part was scanned to measure vessel volume with higher precision. The effective voxel size of the second scanning reached 27.30 μm . The acquisition protocols were as follows: CT scan set-up: total rotation (degrees) = 360, rotation steps = 360; X-ray detector set-up: transaxial = 2048, axial = 2048, exposure time = 1500 ms, binning = 1; system magnification: med-high; X-ray tube set-up: voltage = 80 kV, current = 500 mA. The down-sampling factor used in the reconstruction was 2.

The trabecular bone structure of the patella was different in the anterior, central and subchondral layers (Figure 1(b)). We selected regions of interest (ROIs) from the anterior, central and subchondral sides to compare vessel volume and density (Figure 1(b)). Vessel density was calculated as follows:

$$\text{Vessel density} = \text{vessel volume (cm}^3\text{)} / \text{ROI volume (cm}^3\text{)} \times 100\%.$$

The grayscale ranges for the vessels, trabecular bone and bone marrow were determined by morphological observations. The ranges of vessels were 3400–32,760 Hounsfield unit (HU). The smallest vessels that could be identified were approximately 40 μm in diameter.

2.3. Statistical analysis

Vessel density was analyzed using SPSS 22. Repeated measured one-way analysis of variance (ANOVA) was used to compare the vessel density in the anterior, central and subchondral sides of the patella. A paired *t*-test was used to compare vessel densities between the proximal cartilage-covered portion and the apex and between the anterior and subchondral sides of the medial and lateral apices. A two-tailed *P*-value of <0.05 was considered statistically significant.

3. Results

3.1. Morphological observation

Patellae presented varying degrees of degeneration, with cartilage softening, fissuring and subchondral plate thickening. Despite varying degrees of degeneration, all 13 patellae showed a similar perfusion pattern. The micro-CT results revealed that the patella was mainly perfused by two vessel systems: the prepatellar vascular network and the peripatellar vascular system (Figure 2(a)–(c); Video 1). The locations, intraosseous branches distribution and number of prepatellar vascular networks and peripatellar vascular systems, and their role in intraosseous perfusion were listed in Table 2.

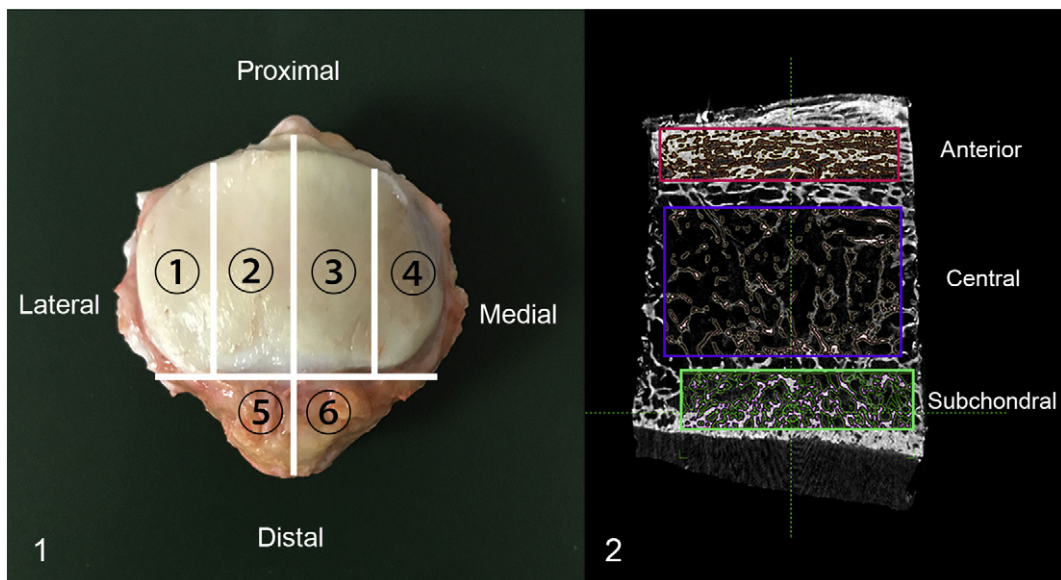


Figure 1. The dividing and regions of interest (ROI) sampling are illustrated. (a) The patella was divided into six parts. These parts were numbered 1–4 in the lateral to medial direction for the proximal cartilage-covered portion and 5 and 6 at the apex. (b) The architecture of the trabecular bone in the sagittal section can be simplified as a “sandwich” structure. ROIs were selected in the anterior, central and subchondral sides, and the vessel density in each ROI was calculated.

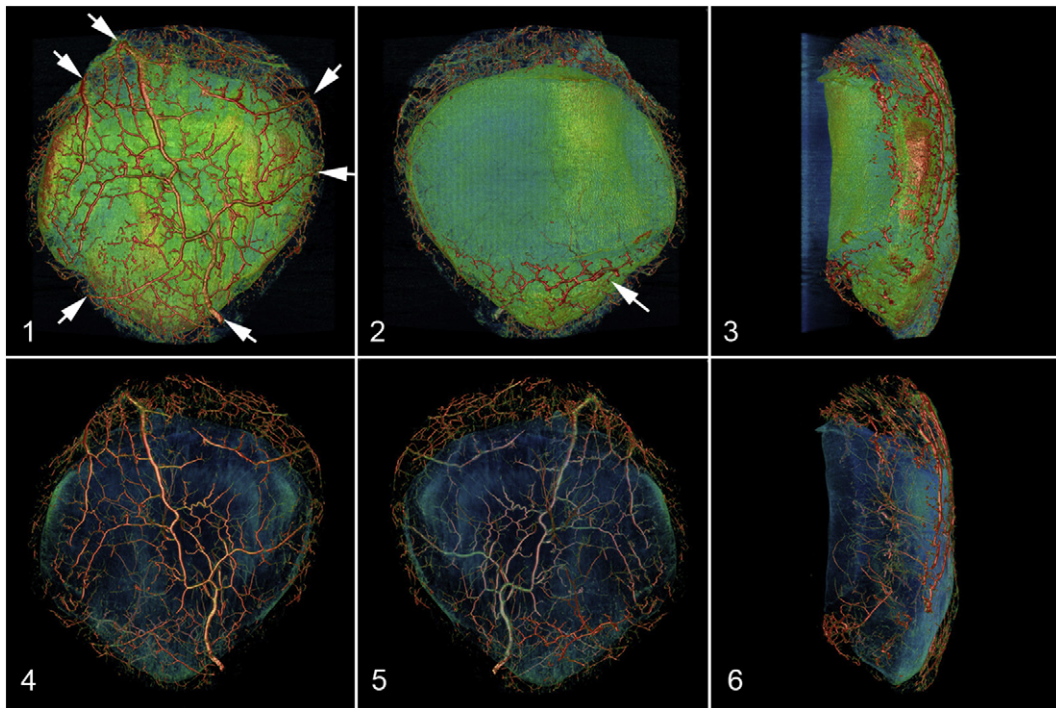


Figure 2. Three-dimensional reconstruction of the patella and its extraosseous and intraosseous vessel systems are shown. Panels (a) and (d), (b) and (e), and (c) and (f) present the anterior, posterior and medial views, respectively. The arrow in (a) indicates the main arteries on the anterior surface, which was anastomosed to form the prepatellar vascular network. The arrow in (b) indicates the arteries in the infrapatellar fat pad (image settings: C = 104, W = 1457, color scheme = hue ramp in (a), (b), (c); C = 1244, W = 3171, color scheme = hue ramp in (d), (e), (f)).

The prepatellar vascular network was located on the anterior surface of the patella, originating from the quadriceps tendon, superficial fascia and medial and lateral retinacula (Figure 3). These arteries were fixed on the anterior periosteum and did not slide during manual movement of the superficial fascia. The prepatellar vascular network gave 18.8 ± 3.1 intraosseous branches, which distributed in the entire patella. Prepatellar vascular network and its intraosseous branches are shown in Figure 4.

The peripatellar vascular system was anastomosed by the arteries in the quadriceps femoris tendon, patellar ligament, retinaculum, infrapatellar fat pad and synovial tissue (Figure 2(b), (c)). There were 5.1 ± 1.8 arteries in the infrapatellar fat pad (Figure 5(a)). Most of the intraosseous branches from the infrapatellar fat pad were short and supplied the apex, and one or two larger arteries extended to the anterior side and subchondral bone (Figure 5(b), (c)). There were abundant arteries in the quadriceps femoris tendon. However, we observed no arteries that penetrated the proximal border of the patella where the quadriceps femoris tendon was attached. There was a tiny gap between the arteries in the tendon and the proximal border of the patella. The arteries within the medial and lateral retinaculum had 1.7 ± 0.8 small, intraosseous branches entering the medial and lateral borders and likely play a limited role in intraosseous perfusion.

3.2. Quantitative analysis

The mean vessel density of the entire patella was $0.41 \pm 0.22\%$. The vessel densities decreased progressively with significant difference ($P < 0.001$) across the anterior, central and subchondral sides, with values of $0.54 \pm 0.29\%$, $0.40 \pm 0.24\%$ and $0.23 \pm 0.19\%$, respectively (Figure 6). This finding was consistent with the distribution of the prepatellar intraosseous vessel branches, suggesting that the prepatellar vascular system was the dominant component of the intraosseous vascularity. Blood perfusion in the four proximal cartilage-covered parts was similar, but the medial and lateral sides of the patellar apex differed in terms of perfusion. The vessel densities of the anterior and subchondral sides of the medial apex were similar ($0.53 \pm 0.58\%$ vs. $0.58 \pm 0.61\%$, n.s.),

Table 2

The location, intraosseous branches distribution and number of prepatellar vascular networks and peripatellar vascular systems, and their role in intraosseous perfusion.

	Location	Intraosseous distribution	Intraosseous branch number	Blood supply
Prepatellar vascular network	Patellar anterior surface	Whole patella	18.8 ± 3.1	Primary
Peripatellar vascular system	Tendons, retinaculum, infrapatellar fat pad	Periphery and apex	Infrapatellar fat pad: 5.1 ± 1.8 Retinaculum: 1.7 ± 0.8	Complementary

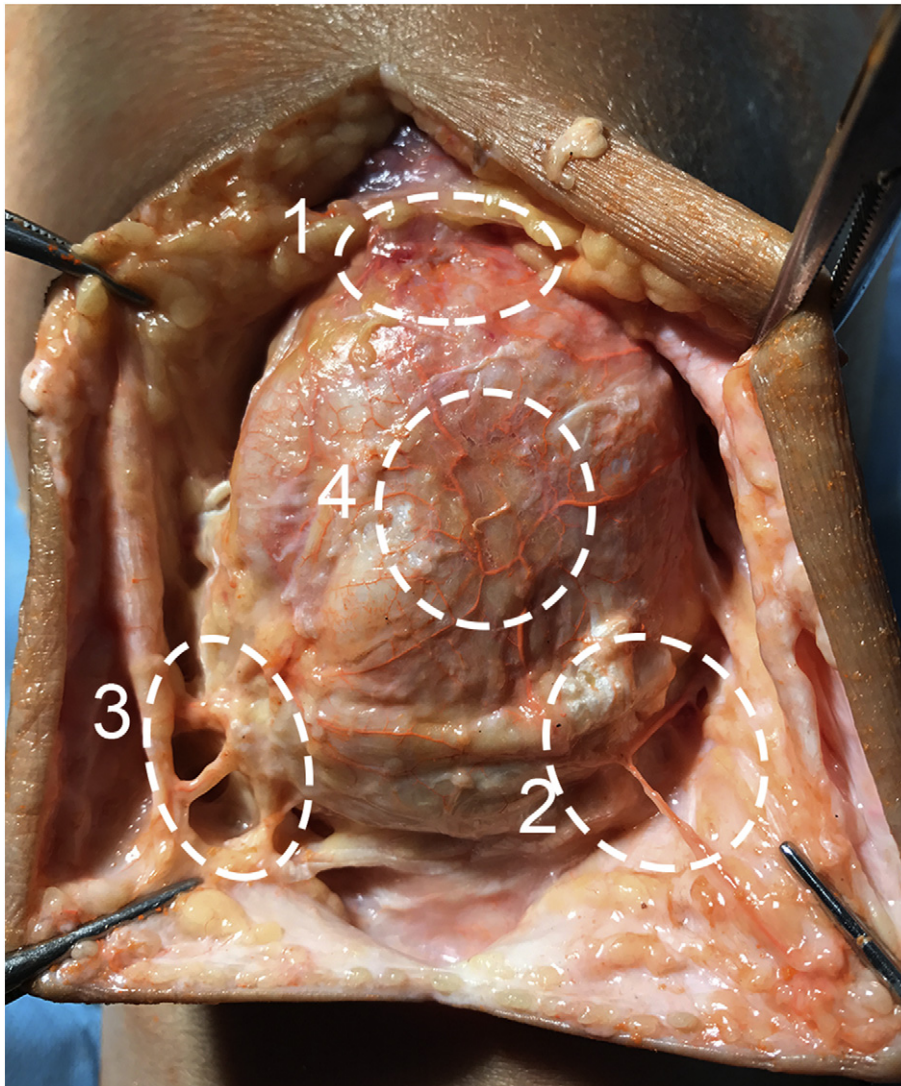


Figure 3. Gross vascular anatomy of the patella is shown. Prepatellar vascular network was well anastomosed with main arteries from multiple directions: quadriceps tendon (1), superficial fascia (2) and lateral retinaculum (3) anastomosed on the anterior surface, forming the prepatellar vascular network (4).

indicating that the medial apex received bilateral perfusion. However, the lateral apex received a greater degree of perfusion from the anterior surface than from the infrapatellar fat pad ($0.59 \pm 0.51\%$ vs. $0.25 \pm 0.24\%$, $P < 0.05$).

4. Discussion

In the present study, we aimed to evaluate the extraosseous and intraosseous vascular anatomy of the patella by micro-CT and present findings relevant to TKA. The most important finding of the present study was that the prepatellar vascular network was well anastomosed with main arteries from multiple directions and served as the dominant blood supply for intraosseous perfusion. Arteries in the infrapatellar fat pad constituted the secondary blood supply and were mainly located at the apex.

Due to its close relationship with TKA, the intraosseous vascularity of the patella has been widely studied [9–11,20]. In the present study, both morphological observations and quantitative analyses revealed that the patella was mainly perfused by the prepatellar vascular network and its intraosseous branches. These results could explain the fact that patellar blood flow decreases significantly during knee flexion and eversion of the patella when the prepatellar vessels are stressed or even stretched [21–23]. Scapinelli [11] reported similar results based on contrast-agent injection and radiography. However, the vascularization of the patella was better than previously reported. We found 18.8 ± 3.1 intraosseous branches from the prepatellar vascular network. Additionally, the prepatellar vascular foramina were located not just in the mid-third of the anterior surface [11] but all over the anterior surface. In the present study, we found 5.1 ± 1.8 intraosseous arteries from the infrapatellar fat pad, which is far fewer than that from the prepatellar vascular network. These arteries were mainly located at the apex, suggesting that the

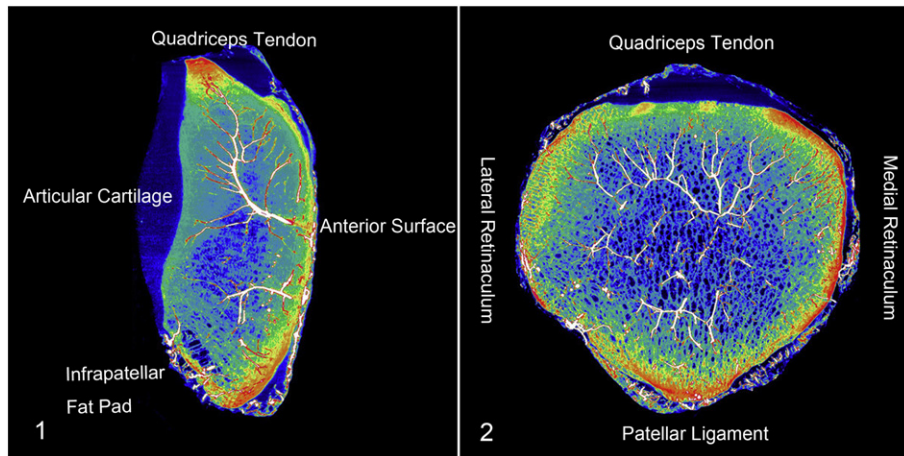


Figure 4. Prepatellar vascular network and its intraosseous branches are shown. (a) Prepatellar vessel branches entered the bone, developed secondary branches, and ultimately reached the articular cartilage. Many vessels with characteristic dendritic-like branches were observed in the middle of the patella where there was more bone marrow and less trabecular bone. A few arteries entered the apex from the infrapatellar fat pad. No arteries entered the patella at the quadriceps tendon and articular cartilage. (b) The branches of the prepatellar vascular network exhibited a radial pattern in the coronal section. Few arteries entered at the medial and lateral retinacula (image settings: C = 490; W = 2091; sky scheme; slice thickness = 2.1 mm).

infrapatellar fat pad is not the major blood supply for the patella. These results are in contrast to Lazaro's conclusions [10]. Using MRI, Lazaro [10] reported that the largest arterial contribution to the patella entered at the distal pole in 100% of specimens and found that an average of 6 ± 2 vessels per specimen penetrated the anterior cortex. These differences might be due to the higher resolution of the micro-CT used in the present study. In fact, we also detected the dominant arteries from the infrapatellar fat pad described by Lazaro [10], but these long arteries were less important than the intraosseous branches from the prepatellar vascular network. Another difference in the findings is that we found few arteries entering the periphery of the patella where the retinaculum and quadriceps tendon are attached. This result is in contrast to Bjorkstrom's results [9] based on X-ray imaging, which might be because X-ray images cannot distinguish the tiny gap between the vessels and the proximal border of the patella.

As the prepatellar vascular network is the major source of intraosseous perfusion, the quadriceps expansion on the patellar anterior surface should be carefully preserved during TKA. Soft-tissue flaps should be kept superficial to the anterior surface, and close exposure and extensive dissection around the patella when approaching the patella should be avoided. Based on the results, Insall's approach involving electrocautery and dissection on the anterior surface of the patella should be avoided because it could greatly damage the prepatellar vascular network and increase the risk of ischemia or even avascular necrosis [24,25]. Our results demonstrate that the dominant prepatellar vascular network had a well-developed anastomosis and that the source vessels came from multiple directions. Thus, blood may still reach the patella when a single medial or lateral incision is performed during TKA. In vivo laser Doppler flowmetry studies also demonstrated that medial and lateral arthrotomy or minimally invasive surgical techniques exert no significant influence on patellar blood flow [21–23]. To better preserve the main arteries of the prepatellar vascular network, we suggest using a wider cuff (possibly wider than 15 mm [8]) when performing capsulotomy.

Lateral reticulum release was performed at TKA for the patients with poor patellofemoral relationships. According to the results of the present study, the procedure might compromise the anastomosed vessel network bilaterally and perfusion is likely reduced. It has been reported that postoperative patella osteonecrosis and fracture following TKA have been associated with a

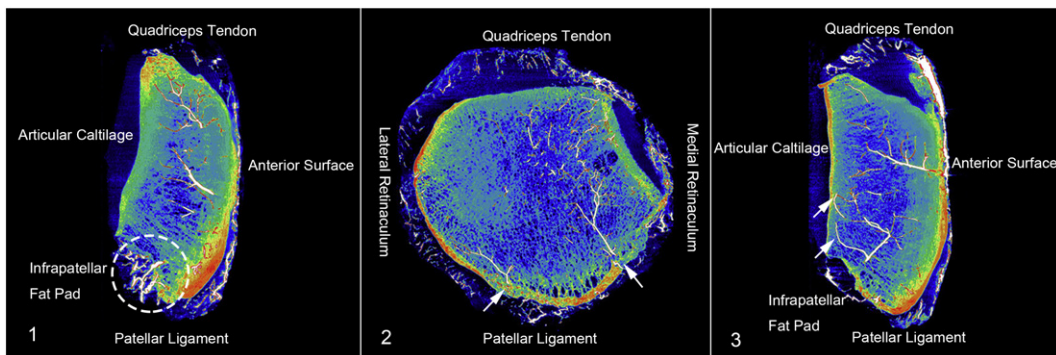


Figure 5. Arteries in the infrapatellar fat pad and its intraosseous branches are shown. (a) Numerous short, curly arteries entered the patellar apex from the infrapatellar fat pad. (b, c) One to two large arteries reached the cartilage and anterior side, as indicated by the arrows.

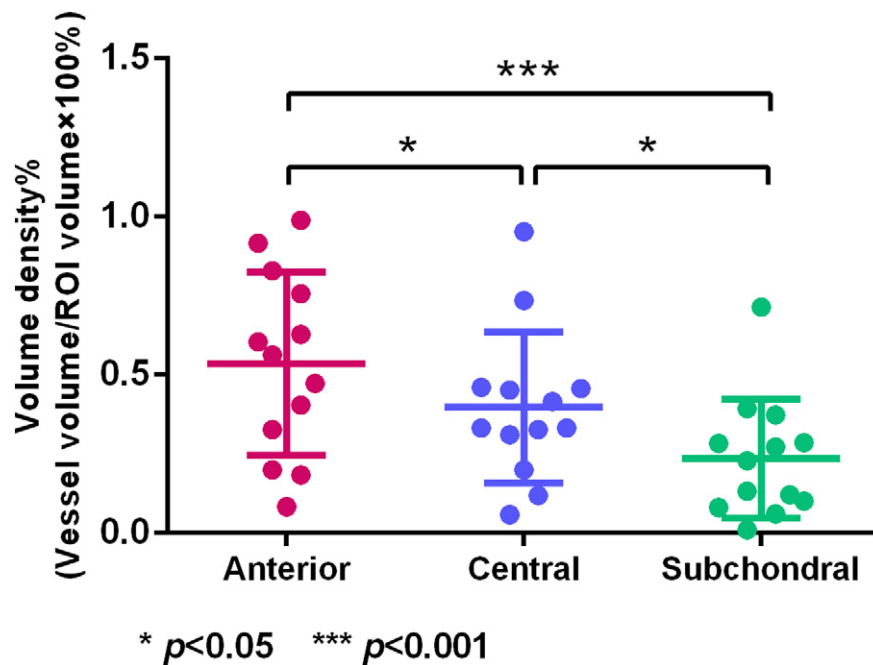


Figure 6. Artery density of the patella decreased from the anterior to the subchondral sides.

lateral release [4–7]. In a large study of 1206 TKAs, Ritter reported that lateral release was associated with significantly more patellar fractures [26]. McMahon [27] revealed an increased incidence of vascular compromise of the patella after lateral release compared with that observed without lateral release. Scintigraphic assessments have also shown an increased incidence of transient patellar hypovascularity associated with lateral release [27,28]. When lateral release is performed and the anterior prepatellar vascular network is poorly perfused, arteries from the infrapatellar fat pad, especially the long arteries, could play a compensatory role. Total infrapatellar fat pad resection or circumferential cauterization after lateral release could further decrease intraosseous perfusion. Thus, the infrapatellar fat pad was recommended to be preserved as much as possible when lateral reticulum release was performed.

The prepatellar vascular network exhibited many dendrite-like branches in the central third of the patella, which could be compromised during patella resection, contributing to periprosthetic patellar fractures after TKA [29,30]. However, there were only terminal arteries in the subchondral area. Resection of 25–30% of the articular side and a five to seven-millimeter thick prosthesis could reduce intraosseous vascular compromise and spare adequate residual bony thickness for revision TKA. In addition, the fixing button should be away from the center of the patella due to the presence of abundant intraosseous arteries at this location (Figure 4(b)). A design with three small pegs should be considered prior to a design with one large central peg to prevent vascular compromise.

To the best of our knowledge, this study constitutes the first 3D visualization and quantification of human patellar intraosseous arteries using micro-CT. The high-resolution images and quantification from this study help us more precisely investigate patellar vascular anatomy. However, there are still some limitations to our study. First, the sample size was relatively small due to the strict exclusion criteria. The specimens were from elderly people with an average age of 63 years and varying degrees of cartilage degeneration. However, age- or degeneration-related vessel changes were not found, and the conclusions might thus be generalizable. Though the blade of the low-speed saw we used was as thin as 500 μm , it was still bigger than small vessels. Thus the ROI was away from the cutting edge, and the vessel density near the sawing site was not measured. The results of the present study might not completely simulate vascular responses, especially during arterial disruption and ischemic injury, as physiologic responses are absent in cadaveric specimens. Although the resolution of the images was 27.30 $\mu\text{m}/\text{voxel}$, the smallest arteries that could be distinguished were 40 μm in diameter because smaller arteries such as capillaries do not exhibit observable contrast against the trabecular bone.

5. Conclusion

The prepatellar vascular network is the dominant blood supply. Close exposure and extensive dissection around the patella should be avoided to preserve the prepatellar vascular network. The infrapatellar fat pad was recommended to be preserved when a lateral reticulum release was performed.

Supplementary data to this article can be found online at <https://doi.org/10.1016/j.knee.2019.02.003>.

Conflicts of interest

The authors have no conflicts of interest to declare.

Acknowledgements

We thank Dr. Duodong Niu and Dr. Qizhao Tan for their excellent technical assistance in the micro-CT operations. We thank Dr. Hanlong Zhen for his contributions to the editing discussion.

Fundings

This work was supported by Peking University Medical and Electronic Foundation (BMU20160600); National Natural Science Foundation of China (11872076 and 31670982); Clinical Medicine Plus X – Young Scholars Project of Peking University (PKU2018LCXQ009); Municipal Natural Science Foundation of Beijing (5184033).

References

- [1] Sharkey PF, Hozack WJ, Rothman RH, Shastri S, Jacoby SM. Insall Award paper. Why are total knee arthroplasties failing today? *Clin Orthop Relat Res* 2002;7–13.
- [2] Doolittle II KH, Turner RH. Patellofemoral problems following total knee arthroplasty. *Orthop Rev* 1988;17:696–702.
- [3] Larson CM, Lachiewicz PF. Patellofemoral complications with the Insall–Burstein II posterior-stabilized total knee arthroplasty. *J Arthroplasty* 1999;14:288–92.
- [4] Insall J, Scott WN, Ranawat CS. The total condylar knee prosthesis. A report of two hundred and twenty cases. *J Bone Joint Surg Am* 1979;61:173–80.
- [5] Scott RD, Turoff N, Ewald FC. Stress fracture of the patella following duopatellar total knee arthroplasty with patellar resurfacing. *Clin Orthop Relat Res* 1982; 147–51.
- [6] Holtby RM, Grosso P. Osteonecrosis and resorption of the patella after total knee replacement: a case report. *Clin Orthop Relat Res* 1996;155–8.
- [7] Noorpuri BS, Maqsood M. Osteonecrosis of the patella and prosthetic extrusion after total knee arthroplasty. *J Arthroplasty* 2002;17:662–3.
- [8] Lazaro LE, Cross MB, Lorich DG. Vascular anatomy of the patella: implications for total knee arthroplasty surgical approaches. *Knee* 2014;21:655–60.
- [9] Bjorkstrom S, Goldie IF. A study of the arterial supply of the patella in the normal state, in chondromalacia patellae and in osteoarthritis. *Acta Orthop Scand* 1980; 51:63–70.
- [10] Lazaro LE, Wellman DS, Klinger CE, Dyke JP, Pardee NC, Sculco PK, et al. Quantitative and qualitative assessment of bone perfusion and arterial contributions in a patellar fracture model using gadolinium-enhanced magnetic resonance imaging: a cadaveric study. *J Bone Joint Surg Am* 2013;95:e1401–7.
- [11] Scapinelli R. Blood supply of the human patella. Its relation to ischaemic necrosis after fracture. *J Bone Joint Surg Br* 1967;49:563–70.
- [12] Ding W-G, Yan W-h, Wei Z-X, Liu J-B. Difference in intraosseous blood vessel volume and number in osteoporotic model mice induced by spinal cord injury and sciatic nerve resection. *J Bone Miner Metab* 2012;30:400–7.
- [13] Qiu X, Shi X, Ouyang J, Xu D, Zhao D. A method to quantify and visualize femoral head intraosseous arteries by micro-CT. *J Anat* 2016;229:326–33.
- [14] van Alphen NA, Morsy M, Laungani AT, Kadar A, Vercnocke AJ, Lachman N, et al. A three-dimensional micro-computed tomographic study of the intraosseous lunare vasculature: implications for surgical intervention and the development of avascular necrosis. *Plast Reconstr Surg* 2016;138:869e–78e.
- [15] Bergeron L, Tang M, Morris SF. A review of vascular injection techniques for the study of perforator flaps. *Plast Reconstr Surg* 2006;117:2050–7.
- [16] Wang DY, Li X, Shen ZC, Gu PL, Pei YR, Zeng G, et al. Three-dimensional architecture of intraosseous vascular anatomy of the hamate: a micro-computed tomography study. *Beijing Da Xue Xue Bao Yi Xue Ban* 2018;50:245–8.
- [17] Xiao Z, Xiong G, Zhang W. New findings about the intrascaphoid arterial system. *J Hand Surg Eur Vol* 2018 Dec;43(10):1059–65.
- [18] Outerbridge RE. The etiology of chondromalacia patellae. *J Bone Joint Surg Br* 1961;43-B:752–7.
- [19] Milz S, Eckstein F, Putz R. The thickness of the subchondral plate and its correlation with the thickness of the uncalcified articular cartilage in the human patella. *Anat Embryol (Berl)* 1995;192:437–44.
- [20] Kayler DE, Lyttle D. Surgical interruption of patellar blood supply by total knee arthroplasty. *Clin Orthop Relat Res* 1988;221–7.
- [21] Kohl S, Evangelopoulos DS, Hartel M, Kohlhof H, Roeder C, Eggli S. Anterior knee pain after total knee arthroplasty: does it correlate with patellar blood flow? *Knee Surg Sports Traumatol Arthrosc* 2011;19:1453–9.
- [22] Hempfing A, Schoeniger R, Koch PP, Bischel O, Thomsen M. Patellar blood flow during knee arthroplasty surgical exposure: intraoperative monitoring by laser doppler flowmetry. *J Orthop Res* 2007;25:1389–94.
- [23] Nicholls RL, Green D, Kuster MS. Patella intraosseous blood flow disturbance during a medial or lateral arthrotomy in total knee arthroplasty: a laser Doppler flowmetry study. *Knee Surg Sports Traumatol Arthrosc* 2006;14:411–6.
- [24] Moreland JR. Mechanisms of failure in total knee arthroplasty. *Clin Orthop Relat Res* 1988;49–64.
- [25] Mochizuki RM, Schurman DJ. Patellar complications following total knee arthroplasty. *J Bone Joint Surg Am* 1979;61:879–83.
- [26] Ritter MA, Herbst SA, Keating EM, Faris PM, Meding JB. Patellofemoral complications following total knee arthroplasty. Effect of a lateral release and sacrifice of the superior lateral geniculate artery. *J Arthroplasty* 1996;11:368–72.
- [27] McMahon MS, Scuderi GR, Glashow JL, Scharf SC, Meltzer LP, Scott WN. Scintigraphic determination of patellar viability after excision of infrapatellar fat pad and/or lateral retinacular release in total knee arthroplasty. *Clin Orthop Relat Res* 1990;10–6.
- [28] Subramanyam P, Sundaram PS, Rao N. Scintigraphic assessment of patellar vascularity in total knee replacement surgeries following lateral release. *Avicenna J Med* 2012;2:54–9.
- [29] Adigweme OO, Sassoon AA, Langford J, Haidukewych GJ. Periprosthetic patellar fractures. *J Knee Surg* 2013;26:313–7.
- [30] Yoo JD, Kim NK. Periprosthetic fractures following total knee arthroplasty. *Knee Surg Relat Res* 2015;27:1–9.